JIN-A02, a Mutant-Selective Fourth-Generation EGFR Inhibitor, Overcomes C797S-Mediated Resistance and Demonstrates Intracranial Activity in NSCLC

Eun Ji Lee[1], Ji Ae Ko[2], Min-je Kim[2], Jae Seok Cho[2], Ji-Youn Han[3], Sang We Kim[4], Ki Hyeong Lee[5], Byoung Yong Shim[6], Jong-Mu Sun[7], Misako Nagasaka[8], Sewon Park[9], Seung Yeon Oh[1], Min Hee Hong[10], Jii Bum Lee[10], Anna Jo[11], Ethan Seah[11], Byoung Chul Cho[10], and Sun Min Lim[10]

ABSTRACT

Purpose: Epidermal growth factor receptor tyrosine kinase inhibitors (EGFR TKI) have revolutionized the treatment of non–small cell lung cancer (NSCLC) with activating *EGFR* mutations. However, acquired resistance—particularly the *EGFR* C797S mutation—remains a major clinical challenge. As no approved targeted therapies are available following disease progression on the third-generation EGFR-TKI osimertinib, this study aimed to evaluate JIN-A02, a novel fourth-generation EGFR-TKI, as a therapeutic strategy to overcome C797S-mediated resistance.

Experimental Design: JIN-A02, a fourth-generation EGFR TKI, was evaluated for its antitumor efficacy and blood–brain barrier penetration in *in vitro* and *in vivo* models of NSCLC harboring *EGFR* C797S and T790M mutations.

Results: JIN-A02 demonstrated potent antiproliferative activity in preclinical NSCLC models harboring *EGFR* C797S and T790M mutations, with superior inhibition of EGFR signaling compared with osimertinib. In both subcutaneous and orthotopic intracranial xenograft models, JIN-A02 elicited substantial tumor regression, indicating robust *in vivo* efficacy. The agent was well tolerated throughout the treatment period without notable toxicity. In line with preclinical data, early clinical trial data showed signs of efficacy, including three patients showing partial response.

Conclusions: These findings highlight JIN-A02 as a promising therapeutic strategy to overcome C797S- and T790M-mediated resistance in *EGFR*-mutant NSCLC, including intracranial disease, and support its further clinical development.

Introduction

Lung cancer is the leading cause of cancer-related mortality worldwide (1). Non–small cell lung cancer (NSCLC), which accounts for approximately 85% of all lung cancer cases, has been associated with poor prognosis, with a 5-year relative survival rate of only 9.7% among patients with distant metastases (2, 3). The epidermal growth factor receptor (EGFR), a critical regulator of cell proliferation and survival, is frequently altered by activating mutations in NSCLC (4, 5). These mutations are identified in 40% to 55% of Asian and 5% to 15% of Western patients (6), with exon 19 deletions and exon 21 L858R substitutions being the most prevalent, accounting for approximately 50% and 40%, respectively, of all EGFR mutations (7).

Phase III clinical trials have shown that first-generation (gefitinib and erlotinib) and second-generation (afatinib) EGFR tyrosine kinase inhibitors (EGFR TKI) significantly improve response rates and progression-free survival (PFS) compared with platinum-based chemotherapy in patients with advanced NSCLC harboring activating *EGFR* mutations (8). However, acquired resistance develops in the majority of patients following an initial response. Among various resistance mechanisms, the *EGFR* T790M mutation is the most prevalent, accounting for approximately 50% to 60% of cases (9). To overcome T790M-mediated resistance, osimertinib, a third-generation EGFR TKI, was developed (10, 11). Osimertinib has shown PFS and overall survival benefit over first- or second-generation TKIs in the FLAURA trial (12). Although it induces strong initial responses, acquired resistance almost inevitably emerges during treatment (13, 14). The most prominent on-target resistance mechanism is the *EGFR* C797S mutation in exon 20, which prevents covalent binding of third-generation EGFR TKIs and confers drug resistance. This mutation is detected in approximately 10% to 26% of patients after second-line therapy and ~7% following first-line osimertinib (15). Mechanistically, substitution of cysteine (Cys797) with serine in the ATP-binding pocket impairs covalent inhibitor binding, thereby reducing drug efficacy (16).

[1]Department of Biomedical Science institute, Graduate School of Medical Science, Brain Korea 21 Project, Yonsei University College of Medicine, Seoul, Republic of Korea. [2]Department of Research Support, Yonsei Biomedical Research Institute, Yonsei University College of Medicine, Seoul, Republic of Korea. [3]Center for Lung Cancer, National Cancer Center - Graduate School of Cancer Science and Policy, Goyang, Republic of Korea. [4]Division of Medical Oncology, Asan Medical Center, University of Ulsan, Seoul, Republic of Korea. [5]Division of Medical Oncology, Chungbuk National University Hospital, Cheongju, Republic of Korea. [6]Department of Medical Oncology, St. Vincent's Hospital, The College of Medicine, The Catholic University of Korea, Seoul, Republic of Korea. [7]Division of Medical Oncology, Samsung Medical Center, Seoul, Republic of Korea. [8]Division of Hematology and Oncology, Department of Medicine, University of California Irvine Medical Center, Orange, California. [9]Yonsei New Il Han Institute for Integrative Lung Cancer Research, Yonsei University of Medicine, Seoul, Republic of Korea. [10]Division of Medical Oncology, Department of Internal Medicine, Yonsei Cancer Center, Yonsei University College of Medicine, Seoul, Republic of Korea. [11]J INTS BIO Inc., Seoul, Republic of Korea.

E.J. Lee and J.A. Ko contributed equally to this article.

Corresponding Author: Sun Min Lim, Division of Medical Oncology, Department of Internal Medicine, Yonsei University College of Medicine, Yonsei Cancer Center, 50-1 Yonsei-Ro, Seodaemun-Gu, Seoul, 03722, Republic of Korea. E-mail: limlove2008@yuhs.ac

Clin Cancer Res 2026;32:1835–45

doi: 10.1158/1078-0432.CCR-25-3720

Translational Relevance

Acquired resistance to third-generation epidermal growth factor receptor tyrosine kinase inhibitors (EGFR-TKI), most commonly driven by the *EGFR* C797S mutation, represents a major unmet clinical need in patients with *EGFR*-mutant non–small cell lung cancer (NSCLC). At present, there are no approved targeted therapies that effectively overcome this resistance mechanism. In this study, we demonstrate that JIN-A02, a fourth-generation EGFR TKI, exhibits robust antitumor activity against *EGFR* C797S mutations across engineered and patient-derived cell lines, as well as in subcutaneous and intracranial xenograft models. In addition, early clinical observations from an ongoing phase I/II study indicate molecular and radiographic responses in patients harboring *EGFR* C797S. Together, these data provide a biological and pharmacologic rationale for the continued clinical development of JIN-A02 as a therapeutic option for patients with *EGFR*-mutant NSCLC.

Currently, no targeted therapies have been approved to effectively overcome resistance mediated by the *EGFR* C797S mutation. After disease progression on osimertinib, platinum-based cytotoxic chemotherapy remains the standard of care, despite its considerable toxicities, including immunosuppression, myelosuppression, and hepatotoxicity. Moreover, many patients develop compound *EGFR* C797S mutations, for which no existing treatment can effectively suppress multiple concurrent resistance mechanisms (17). Thus, the development of next-generation EGFR TKIs capable of selectively targeting *EGFR* C797S and its associated alterations constitutes a critical unmet clinical need in *EGFR*-mutant NSCLC.

JIN-A02 is a novel, orally available fourth-generation EGFR TKI that selectively and reversibly inhibits resistance-associated *EGFR* mutations, including C797S and T790M. In this study, we demonstrated its potent, dose-dependent antitumor activity in cell lines and xenograft models harboring these mutations. Notably, JIN-A02 crosses the blood–brain barrier (BBB) and exerts robust efficacy in intracranial tumor models. These findings support JIN-A02 as a promising therapeutic strategy for patients with EGFR TKI–resistant NSCLC driven by C797S or T790M mutations. In this study, we present preclinical and early clinical trial results of JIN-A02.

Materials and Methods

Chemicals and antibodies

Osimertinib was purchased from Selleckchem. JIN-A02 was provided by J INTS BIO.

Antibodies were obtained from the following manufacturers: phospho-EGFR (Tyr1068; no. 2234, RRID: AB_331701), EGFR (no. 4267, RRID: AB_2895042), phospho-ERK1/2 (Thr202/Tyr204; no. 4370, RRID: AB_2315112), ERK1/2 (no. 4696, RRID: AB_390780), phospho-AKT (Ser473; no. 9271, RRID: AB_329825), AKT (no. 9272, RRID: AB_329827), phospho-S6K (no. 4858, RRID: AB_916156), and S6K (no. 2217, RRID: AB_331355) were all purchased from Cell Signaling Technology. β-Actin (no. A3854, RRID: AB_262011) was purchased from Sigma.

Cell culture

PC9 (RRID: CVCL_B260), HCC827 (RRID: CVCL_2063), and H1975 (RRID: CVCL_1511) were purchased from the ATCC, and Ba/F3 cells (ACC300) were purchased from the Leibniz Institute DSMZ (German Collection of Microorganisms and Cell Cultures GmbH). Cells were maintained in RPMI-1640 medium supplemented with 10% FBS and 1% antibiotics in an incubator at 37°C with 5% CO_2. Culture medium was refreshed every 2 days, and cells were passaged once or twice per week depending on the proliferation rate of each cell line. All cell lines were routinely tested and confirmed to be negative for *Mycoplasma* contamination using the Myco-Read Mycoplasma Detection Kit (Biomax).

Ba/F3 cells expressing EGFR mutations

Ba/F3 cells were transduced with lentiviral particles encoding human wild-type (WT) or mutant *EGFR* sequences cloned into the pLVX-puro vector (RRID: Addgene_125839). The pLVX-puro vector contains a cytomegalovirus promoter to drive the expression of the transgene and a puromycin resistance gene under the PGK promoter, enabling efficient antibiotic selection. Stable cell lines were established by puromycin selection (1 μg/mL). Transduced Ba/F3 cells were cultured under standard conditions. On the other hand, the *EGFR* WT Ba/F3 cell lines were cultured in growth medium supplemented with human recombinant EGF (10 ng/mL, R&D Systems) and puromycin (0.5 μg/mL).

Generation of PC9_DC cells via CRISPR/Cas9

The PC9_DC (*EGFR* E19del/C797S) cell line was generated by introducing the C797S mutation into PC9 cells already carrying the *EGFR* E19del mutation using CRISPR/Cas9 genome editing. The CRISPR/Cas9 plasmid (no. 632601) was purchased from Clontech Laboratories, Inc., and the single-guide RNA (sgRNA) and single-stranded oligonucleotide (ssODN) repair template were synthesized by Macrogen (RRID: SCR_014454). In this system, Cas9, guided by the sgRNA (5′-GCTGCCTCCTGGACTATGTC-3′), introduced a double-strand break at the target locus, allowing homology-directed repair using the ssODN template (5′-TGTGCCGCCTGCTGGGCATCTGCCTCACCTCCACCGTGCAACTCATCACGCAGCTCATGCCCTTCGGCAGCCTCCTGGACTATGTCCGTGAACACAAAGACAATATTGGCTCCCAGTACC-3′) encoding the C797S mutation. After genome editing, single-cell cloning and stepwise validation were conducted to confirm the successful incorporation of the dual *EGFR* mutations. The resulting cell line was designated as PC9_DC.

Establishment of patient-derived preclinical models

Patient-derived cell lines (PDC; YU-1097, YU-1182, and YUX-1024) were established from malignant pleural effusions, as previously described (18), and are not associated with RRIDs. PDCs were cultured using standard methods and used within 40 passages. Flow cytometry with EpCAM staining confirmed >99% EpCAM-positive cells, indicating high epithelial tumor cell content. Genomic fidelity to the original tumors was confirmed by Sanger and whole-exome sequencing (WES; Supplementary Table S1).

Cell viability assays

Cells were seeded in 96-well plates at a density of 2×10^3 cells per well and incubated overnight at 37°C to allow adherence. JIN-A02 and the comparator drug osimertinib were added at the indicated concentrations and incubated for 72 hours. Cell viability was assessed using the CellTiter-Glo Luminescent Cell Viability Assay

(Promega), according to the manufacturer's instructions. Dose–response curves, IC_{90}, and AUC values were determined using GraphPad Prism software (RRID: SCR_002798). All experiments were independently performed at least three times.

Colony formation assay

Cells were seeded in six-well plates and cultured in growth medium. After initial attachment, the medium was replaced every 3 days with fresh medium containing the indicated compounds. After 14 days of drug treatment, colonies were fixed with 4% paraformaldehyde and stained with 0.5% crystal violet for 1 hour at room temperature. Plates were gently washed with distilled water and air-dried before imaging.

Immunoblot analysis

Immunoblotting was performed to assess the phosphorylation status of kinases and the total protein levels of target molecules. Protein lysates were separated by SDS-PAGE and transferred onto nitrocellulose membranes. Membranes were blocked in 5% skim milk in TBS with Tween 20 and incubated with the indicated primary antibodies, followed by horseradish peroxidase (HRP)–conjugated secondary antibodies. β-Actin was used as a loading control. Chemiluminescent signals were detected using the SuperSignal West Pico Chemiluminescent Substrate (Thermo Fisher Scientific) and visualized by exposure to X-ray film in a dark room.

In vivo studies

All animal experiments were conducted in accordance with institutional guidelines and approved by the Institutional Animal Care and Use Committee of Yonsei University College of Medicine. The facility is fully accredited by the Association for Assessment and Accreditation of Laboratory Animal Care International. Mice were housed under specific pathogen-free conditions with no more than five animals per cage, and animal welfare (including food, water, and hygiene) was monitored daily. Female mice were used for all *in vivo* experiments for consistency across treatment groups.

To establish patient-derived xenograft models, YU-1097 cells (5×10^6 in 100 μL PBS) were subcutaneously implanted into the flanks of 6-week-old female BALB/c nude mice (Orient Bio Inc., RRID: IMSR_RJ:BALB-C-NUDE). Once tumors reached an average volume of 200 mm^3, mice were randomized (at least five mice per group) to receive one of the following treatments via oral administration: (i) vehicle control, (ii) osimertinib (25 mg/kg, once daily), (iii) JIN-A02 (10 mg/kg, once daily), or (iv) JIN-A02 (30 mg/kg, once daily).

Tumor size was measured three times weekly using digital calipers and calculated as $0.532 \times \text{length} \times \text{width}$. Percent tumor volume change was calculated as $(V_t - V_0)/V_0 \times 100$. Tumor growth inhibition (TGI) was calculated using two formulas described by Drilon and colleagues (19):

$$\text{If } V_t > V_0,\ TGI = 100 \times [1 - (V_t - V_0 / CV_t - CV_0)]$$

$$\text{If } V_t < V_0,\ TGI = 100 \times [2 - (V_t - V_0)]$$

in which V_0 and V_t represent tumor volumes at baseline and study endpoint in the treatment group and CV_0 and CV_t denote the corresponding volumes in the control group. Tumor measurements were performed by a single investigator who was unaware of the treatment group assignments.

No animals were excluded from the analysis, and all enrolled mice completed the planned treatment and evaluation schedule.

Intracranial tumor model

Intracranial tumor models were established by stereotactic implantation of YU-1097-luc cells or PC9-luc cells into the right frontal lobe of 6-week-old female BALB/c nude mice. Mice were anesthetized and positioned in a stereotactic apparatus. A 0.5-mm burr hole was drilled into the right frontal bone, and a guide screw was inserted. A total of 5×10^5 cancer cells suspended in 5 μL PBS were injected over 5 minutes through the guide screw using a microsyringe at a depth of 2.5 mm. The skin incision was closed using surgical glue.

Tumor growth was monitored using the IVIS Spectrum System (Xenogen, PerkinElmer). Mice were intraperitoneally injected with 150 mg/kg D-luciferin, and imaging was performed 15 minutes after injection using Living Image software (PerkinElmer, RRID: SCR_014247). One week after tumor implantation, mice exhibiting detectable bioluminescent signals were randomized ($n = 12$ per group) to receive one of the following oral treatments: (i) vehicle control, (ii) osimertinib (25 mg/kg, once daily), or (iii) JIN-A02 (30 mg/kg, once daily).

Immunohistochemistry

Immunohistochemistry (IHC) was performed on 4-μm-thick formalin-fixed, paraffin-embedded tissue sections. Slides were heat-treated and deparaffinized in xylene, followed by rehydration through graded alcohols. Antigen retrieval was carried out in 1 mmol/L EDTA buffer (pH 8) at 125°C for 30 seconds. Slides were then pretreated with a peroxidase-blocking reagent (Dako) for 5 minutes and washed with 50 mmol/L Tris-Cl (pH 7.4). Nonspecific binding was blocked with normal goat serum (Dako), after which slides were incubated for 1 hour with an anti-Ki67 antibody (no. 9027, Cell Signaling Technology, RRID: AB_2636984). Slides were washed with 50 mmol/L Tris-Cl (pH 7.4) and incubated for 30 minutes with SignalStain Boost IHC detection reagent (HRP, rabbit; no. 8114; Cell Signaling Technology, RRID: AB_10544930). After additional washes, immunoperoxidase staining was developed for 5 minutes with 3,3′-diaminobenzidine (DAB; Dako). Slides were counterstained with hematoxylin, dehydrated through graded alcohols and xylene, mounted, and coverslipped. Histoscore (H-score) was calculated by inForm 2.6 Tissue Analysis Software (Akoya Biosciences, RRID: SCR_019155).

Whole exome sequencing

Genomic DNA purity and concentration were measured using the PicoGreen dsDNA assay (Invitrogen) and agarose gel electrophoresis. A genomic fragment library was prepared using the SureSelect v5 Kit (Agilent Technologies) for whole exome sequencing (WES) on the Illumina HiSeq 2500 platform. Sequencing reads were aligned to the human reference genome (hg19) using the Burrows–Wheeler Aligner (RRID: SCR_010910), and postalignment processing was performed with the Genome Analysis Toolkit. Somatic variants were detected with Mutect2 (RRID: SCR_026692) and annotated using Oncotator (RRID: SCR_005183). After sequencing, 171 cancer-associated genes were analyzed.

Statistical analysis

Statistical analyses were performed using GraphPad Prism (version 7). *In vitro* experiments were independently repeated at least three times with technical triplicates. Data are presented as mean ± SEM for cell-based assays and mean ± SD for animal studies. Group comparisons were made using two-way ANOVA with a Bonferroni *post hoc* test or Kruskal–Wallis with a Dunn test, as appropriate.

$P < 0.05$ was considered statistically significant. Sample size was determined based on prior experience with similar xenograft models and was sufficient to detect biologically meaningful differences between treatment groups.

Patients

All patient samples were obtained from patients with *EGFR*-mutant NSCLC treated at Severance Hospital, Yonsei University, either before or after disease progression on EGFR TKI therapy. The study was approved by the Institutional Review Board of Severance Hospital (no. 4-2016-0001), and all patients provided written informed consent. This study was conducted in accordance with the ethical principles of the Declaration of Helsinki (World Medical Association) and the Belmont Report (U.S. Department of Health and Human Services).

Phase I study of JIN-A02

The first-in-human phase I study was conducted to evaluate the safety of JIN-A02, including a dose-escalation phase, to characterize dose-limiting toxicities (DLT) and determine the recommended phase II dose (NCT05394831); preliminary data have been presented elsewhere (20–27). Key eligibility criteria included advanced-stage NSCLC with an activating *EGFR* mutation and disease progression on at least one prior EGFR inhibitor. A measurable lesion was required for exploratory evaluation of efficacy. Starting from 12.5 mg once daily, JIN-A02 dose levels were escalated after evaluating dose–DLT relationships and toxicity probabilities during the first 21 days of dosing. Blood sampling for ctDNA testing was performed at screening, 4 weeks, and end of treatment (EoT). Intrapatient dose escalation to the next dose level was allowed. The trial was conducted in accordance with the Declaration of Helsinki and Good Clinical Practice guidelines. All applicable regulatory requirements were fulfilled, and the protocol was approved by an Ethics Committee at all participating sites. All participants provided written informed consent before undergoing any study procedures or sharing any data, imaging, and tissue for the study.

Results

JIN-A02 exhibits potent *in vitro* activity against *EGFR* C797S–driven resistance models

To evaluate the *in vitro* efficacy of JIN-A02 against C797S-mediated EGFR resistance, we established a panel of Ba/F3 cell lines harboring clinically relevant *EGFR* mutations (**Table 1**; Supplementary Fig. S1A–S1D). These included *EGFR* E19del/C797S and *EGFR* L858R/C797S, which reflect resistance mechanisms following first-line osimertinib therapy, as well as *EGFR* E19del/T790M/C797S and *EGFR* L858R/T790M/C797S, modeling resistance that arises after second-line osimertinib treatment. Cell viability assays were conducted using these engineered Ba/F3 cells, with osimertinib included as a reference comparator. We used IC_{90} as it more accurately reflects the inhibition level associated with meaningful antitumor effects. JIN-A02 exhibited potent antiproliferative activity across all tested models, with IC_{90} values of 117 nmol/L (*EGFR* E19del/C797S), 231 nmol/L (*EGFR* L858R/C797S), 192 nmol/L (*EGFR* E19del/T790M/C797S), and 359 nmol/L (*EGFR* L858R/T790M/C797S; Supplementary Fig. S1A–S1D). Immunoblot analysis demonstrated that JIN-A02 substantially inhibited EGFR phosphorylation in all C797S-mutant models, even upon long exposure observation, corroborating its target-specific activity (Supplementary Fig. S1E–S1H). Furthermore, JIN-A02 demonstrated antiproliferative activity comparable with that of osimertinib in Ba/F3 cells engineered to express *EGFR* E19del, *EGFR* L858R, *EGFR* E19del/T790M, and *EGFR* L858R/T790M mutations (Supplementary Fig. S2A).

JIN-A02 demonstrates potent antitumor activity in *EGFR* C797S preclinical models, including PDCs

To validate the findings from Ba/F3 models, we evaluated the antitumor efficacy of JIN-A02 in patient-derived tumor cell lines harboring *EGFR* C797S and in additional models harboring *EGFR* activating mutations and *EGFR* T790M (**Table 2**; Supplementary Fig. S2B and S3A–S3C).

YU-1097 is a PDC established from the pleural effusion of a patient initially harboring an *EGFR* E19del mutation. Following progression on first-line gefitinib and subsequent osimertinib treatment, the tumor acquired *EGFR* T790M and C797S mutations, resulting in an *EGFR* E19del/T790M/C797S genotype. JIN-A02 demonstrated potent antiproliferative activity in this model, with an IC_{90} of 624 nmol/L, whereas osimertinib failed to achieve 90% growth inhibition at the highest concentration (1,000 nmol/L), precluding IC_{90} determination, and resulted in a maximum growth inhibition of approximately 74.2% (Supplementary Fig. S3A). PC9_DC cells were generated via CRISPR/Cas9-mediated knock-in of the *EGFR* C797S mutation into parental PC9 cells harboring *EGFR* E19del. Similarly, IC_{90} values for osimertinib could not be determined in PC9 and PC9_DC cells because 90% growth inhibition was not achieved at concentrations up to 1,000 nmol/L, with maximum growth inhibition of approximately 19.3% and 63.4%, respectively. In contrast to osimertinib, JIN-A02 retained potent

Table 1. Cell viability for treatment of JIN-A02 in Ba/F3 cell lines with EGFR mutations and WT.

	IC_{90} nmol/L								
Compound	**D**	**L**	**DT**	**LT**	**DC**	**LC**	**DTC**	**LTC**	**WT[a]**
Osimertinib	6	7	5	8	398	ND (12.1%[b])	ND (64.2%[b])	ND (68.2%[b])	295
JIN-A02	76	86	56	45	117	231	192	359	ND (17.6%[c])

Abbreviations: D, E19del; L, L858R; T, T790M; C, C797S; ND, not detected; WT, wild-type.
[a]Supplemented with recombinant human EGF (10 ng/mL).
[b]Cell viability at 1,000 nmol/L osimertinib.
[c]Cell viability at 1,000 nmol/L JIN-A02.

Table 2. Cell viability for treatment of JIN-A02 in NSCLC and PDCs with EGFR mutations containing C797S.

	IC_{90} nmol/L				
Compound	**PC9 (D)**	**YUX-1024 (L)**	**H1975 (LT)**	**PC9_DC (DC)**	**YU-1097 (DTC)**
Osimertinib	ND (19.3%[a])	ND (34.5%[a])	ND (33.8%[a])	ND (63.4%[a])	ND (69.2%[a])
JIN-A02	229	501	245	275	624

Abbreviations: D, E19del; L, L858R; T, T790M; C, C797S; ND, not detected.
[a]Cell viability at 1,000 nmol/L osimertinib.

antiproliferative activity in both cell lines, with IC_{90} values of 229 nmol/L and 275 nmol/L, respectively (Supplementary Fig. S3B). Moreover, JIN-A02 showed robust IC_{90} and AUC values in *EGFR* activating mutation cell lines, including HCC827 (*EGFR* E19del), PDC YUX-1024 (*EGFR* L858R), and T790M harboring H1975 (*EGFR* L858R/T790M; **Table 2**; Supplementary Fig. S2B; Supplementary Table S2).

To assess the effects of JIN-A02 under long-term exposure, we performed colony formation assay in *EGFR* C797S–harboring models. In YU-1097 (*EGFR* E19del/T790M/C797S), JIN-A02 at 10 nmol/L markedly reduced colony number and size and at 30 nmol/L nearly abolished colonies. A similar pattern was observed in PC9_DC (*EGFR* E19del/C797S), in which JIN-A02 at 10 or 30 nmol/L visibly decreased clonogenic growth. In YU-1182 (*EGFR* L858R/C797S), although 90% growth inhibition was not achieved in short-term viability assays at concentrations up to 1,000 nmol/L (Supplementary Fig. S3C), prolonged exposure reduced colony number and size with JIN-A02 at 10 or 30 nmol/L. By contrast, colonies persisted with osimertinib at 30 or 100 nmol/L in all *EGFR* C797S–harboring cell lines. (Supplementary Fig. S3D–S3F).

In addition, immunoblot analysis revealed dose-dependent inhibition of EGFR phosphorylation and downstream signaling phosphorylation by JIN-A02 in all *EGFR* C797S–harboring models. In contrast, osimertinib failed to suppress EGFR phosphorylation and downstream signaling (Supplementary Fig. S3G–S3I).

Efficacy of JIN-A02 in a triple-mutant *EGFR* E19del/T790M/C797S xenograft model

To assess the *in vivo* efficacy of JIN-A02 against *EGFR* C797S–mediated resistance, we established a xenograft model using YU-1097 cells harboring *EGFR* E19del/T790M/C797S. Mice were administered vehicle, osimertinib (25 mg/kg), or JIN-A02 (10 or 30 mg/kg) orally once daily. Consistent with *in vitro* results, JIN-A02 induced robust and durable tumor regression, resulting in TGI rates of 115.9% and 168.2% at 10 and 30 mg/kg, respectively, whereas osimertinib achieved a TGI of 49.3% (**Fig. 1A**). No significant changes in body weight were observed throughout the treatment period (**Fig. 1B**). On day 29, waterfall plot analysis revealed that the majority of mice treated with JIN-A02 exhibited tumor shrinkage. By contrast, most animals in the vehicle and osimertinib groups showed progressive disease (PD; **Fig. 1C**). IHC of xenograft tumors showed intense p-EGFR staining and numerous Ki67-positive nuclei in vehicle-treated samples. Treatment with JIN-A02 at 30 mg/kg led to a significant reduction in the H-scores of phosphor-EGFR and Ki67 in tissue sections, with decreases of 70% and 52%, respectively, compared with the vehicle group (**Fig. 1D** and **E**). These results demonstrate that JIN-A02 effectively inhibited *EGFR* E19del/T790M/C797S activation *in vivo*, resulting in significant tumor suppression of YU-1097.

JIN-A02 confers intracranial efficacy in an *EGFR* C797S brain metastasis model

Brain metastases are observed in approximately 20% to 25% of patients with *EGFR*-mutant NSCLC at diagnosis and increase in frequency with disease progression. Thus, the ability of EGFR TKIs to penetrate the BBB and achieve sufficient intracranial exposure is critical for improving clinical outcomes. To assess the intracranial efficacy of JIN-A02, we established an orthotopic brain metastasis model by directly injecting YU-1097 cells harboring *EGFR* E19del/T790M/C797S into the mouse brain. Bioluminescence imaging demonstrated that JIN-A02 (30 mg/kg, orally, once daily) rapidly reduced tumor signals by week 1 and maintained sustained suppression through week 4 (**Fig. 2A**). Quantitative analysis confirmed significant inhibition of tumor growth by JIN-A02 compared with vehicle and osimertinib (25 mg/kg; **Fig. 2B**). No significant changes in body weight were observed in any treatment group (**Fig. 2C**). On day 28, waterfall plot analysis showed tumor progression in most mice receiving vehicle or osimertinib, whereas nearly all JIN-A02–treated mice exhibited tumor regression (**Fig. 2D**). Histopathologic analysis further confirmed marked reduction of intracranial tumor lesions in the JIN-A02 group, whereas substantial tumor burdens remained in the control groups (**Fig. 2E**). Furthermore, JIN-A02 showed antitumor activity comparable with osimertinib in the PC9 intracranial model (Supplementary Fig. S4A and S4B).

JIN-A02 shows early signs of efficacy in phase I/II trial

As of the data cutoff date (July 22, 2025), 23 patients have been treated with JIN-A02 with a once-daily schedule in part A dose-escalation cohort (**Fig. 3**). The median age was 64 years (range, 52–78 years) and the proportion of female patients was 56.5% (Supplementary Table S3). JIN-A02 has demonstrated good overall tolerance and a safety profile (Supplementary Table S4). The longest duration of treatment was 651 days in an *EGFR* E19del/T790M/C797S patient (initial dose: 25 mg and current dose: 150 mg). There were three patients with partial response (PR) and seven patients with stable disease (SD). Three PRs were observed in the 50, 100, and 300 mg cohorts, respectively. In the 300 mg cohort, one patient's target lesion size was reduced by 39.7% at cycle 3 day 1 and cycle 5 day 1 and by 44.9% at cycle 7 day 1 compared with baseline (**Fig. 4A**). In this patient, the size of brain metastasis also reduced by 25% at cycle 5 day 1 and cycle 7 day 1 (**Fig. 4B**). Exploratory ctDNA analyses were conducted in a subset of participants as this assessment was incorporated mid-phase. These favorable clinical findings

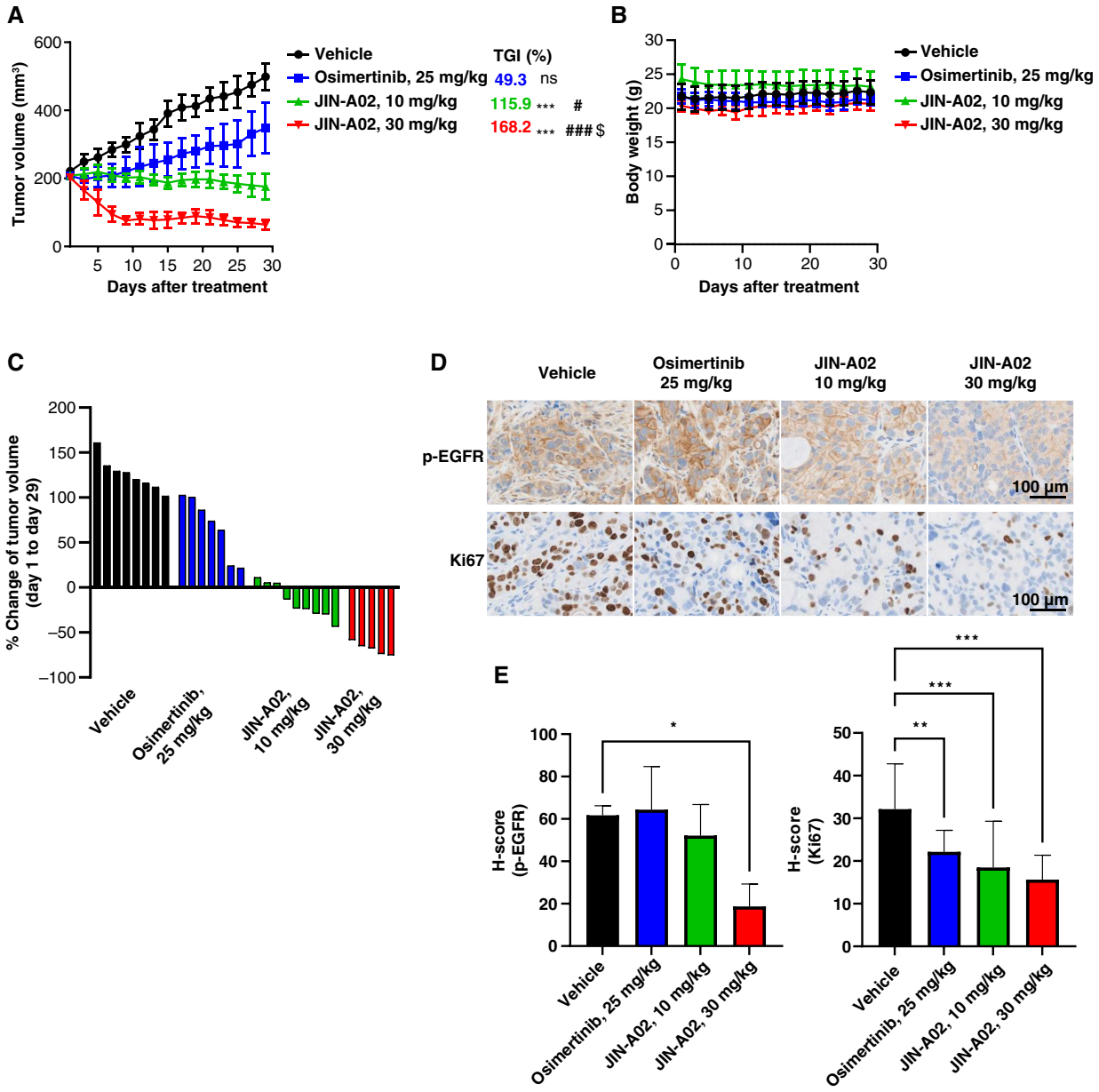

Figure 1.

In vivo activity of JIN-A02 in EGFR C797S–mediated osimertinib-resistant models. **A,** Tumor growth curve of YU-1097 xenografts in response to JIN-A02. Statistical analysis was performed using Kruskal–Wallis with a Dunn *post hoc* test: ***, $P < 0.001$ versus vehicle; #, $P < 0.05$ versus osimertinib; ###, $P < 0.001$ versus osimertinib; $, $P < 0.05$ versus JIN-A02 10 mg/kg; ns, not significant. Data represent the means ± standard deviation. **B,** Body weight of the mice during the experimental period. **C,** Waterfall plot representing the percentage of tumor volume change in mice after 4 weeks of treatment with the indicated drugs. **D,** Representative images of IHC staining for p-EGFR and Ki67 of tumor sections. **E,** H-score for phospho-EGFR and Ki67 of tumor sections. Statistical analysis was performed using one-way ANOVA, with a Tukey honest significant difference *post hoc* test: ***, $P < 0.001$ versus vehicle; **, $P < 0.01$ versus vehicle; *, $P < 0.05$ versus vehicle. Data represent the means ± standard deviation. p-EGFR, phosphorylated EGFR.

align with the molecular effects of JIN-A02 observed in the ctDNA analysis, which demonstrated complete clearance of C797S and E19del and reduction of T790M after JIN-A02 treatment (**Fig. 4C**). In the 300 mg cohort, one SD patient exhibited detectable E19del ctDNA at cycle 1 day 1, which became undetectable at EoT. Within the same cohort, two PD patients also demonstrated reductions in *EGFR*-mutant ctDNA; however, both individuals carried baseline *TP53* co-mutations (variant allele frequency of 12.63% and 3.84%, respectively; Supplementary Fig. S5). These observations indicate that although JIN-A02 produced molecular activity against *EGFR* mutations, disease progression in these patients may have been influenced by non-*EGFR* co-mutations such as *TP53*. In the pharmacokinetic analysis, the plasma concentration of JIN-A02 reached a relatively steady state for a certain period after dosing, suggesting

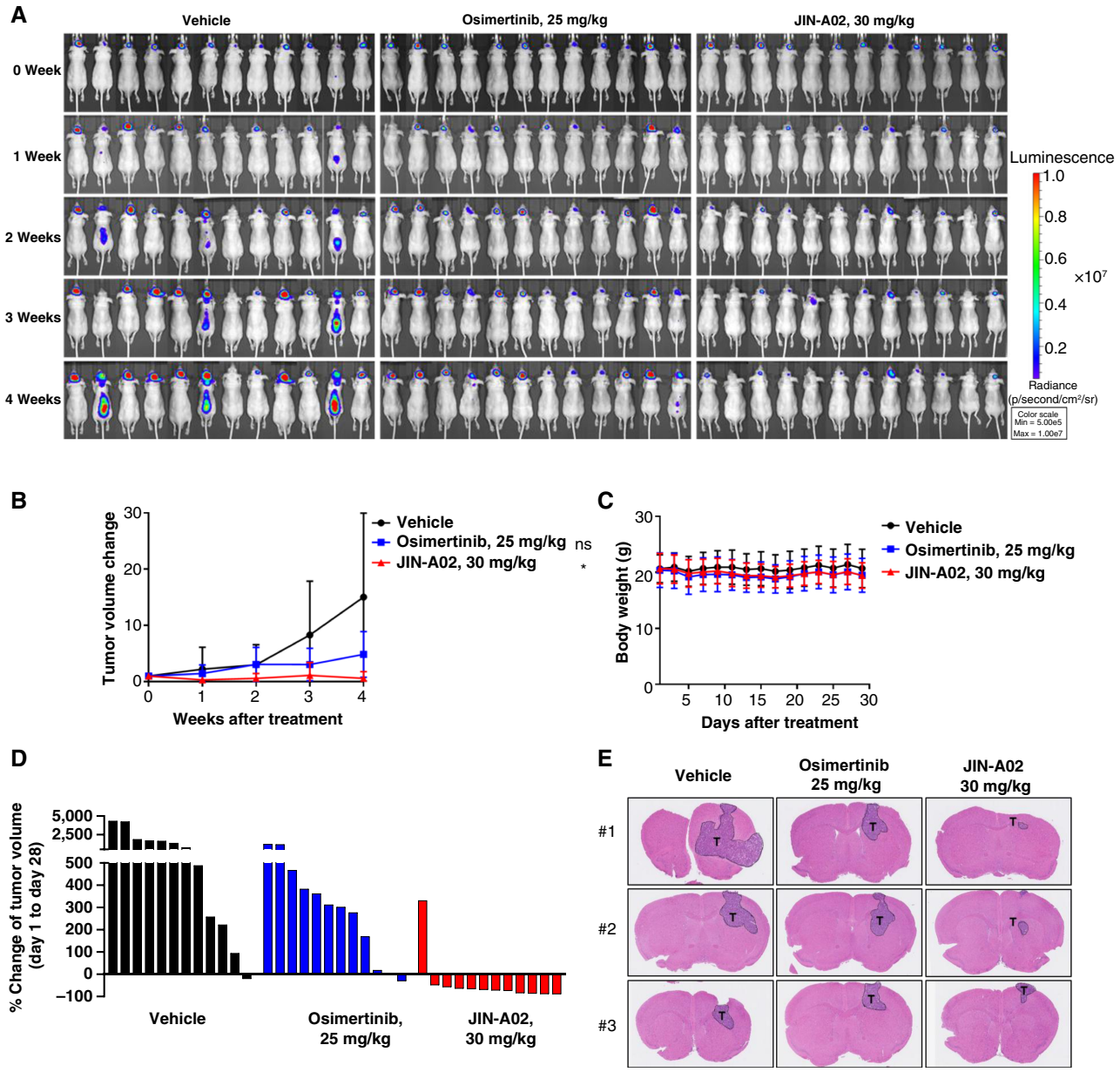

Figure 2.

Antitumor activity of JIN-A02 in YU-1097 cell–driven intracranial tumor models. **A,** IVIS imaging of intracranial YU-1097-luc tumors following treatment with osimertinib and JIN-A02. **B,** Change in tumor burden derived from bioluminescent signal. Statistical analysis was performed using Kruskal–Wallis with a Dunn *post hoc* test: *, $P < 0.05$ versus vehicle. Data represent the means ± standard deviation. **C,** Body weight of the mice during the experimental period. **D,** Waterfall plot representing the percent change in tumor burden after 4 weeks of the indicated treatments. **E,** Representative image of hematoxylin and eosin staining of brain slices at the EoT. H&E, hematoxylin and eosin. T, tumor region.

drug accumulation and the potential for more stable plasma levels with repeated administration (**Fig. 4D**). A reduction in brain metastases was first observed at the 100 mg dose. Part of the brain lesions showed complete disappearance in another 300 mg cohort patient. Treatment-related adverse events of grade 3 occurred in two patients (Supplementary Table S4). Gastrointestinal toxicities (e.g., diarrhea, nausea, and vomiting) were the most common adverse events. Skin toxicities were mild and no grade 3 or higher events have been reported. At the data cutoff date, dose escalation is ongoing at 300 mg once daily.

Discussion

On-target resistance mediated by the *EGFR* C797S mutation remains a major clinical challenge in the management of *EGFR*-mutant NSCLC (15, 28, 29). This mutation disrupts the covalent

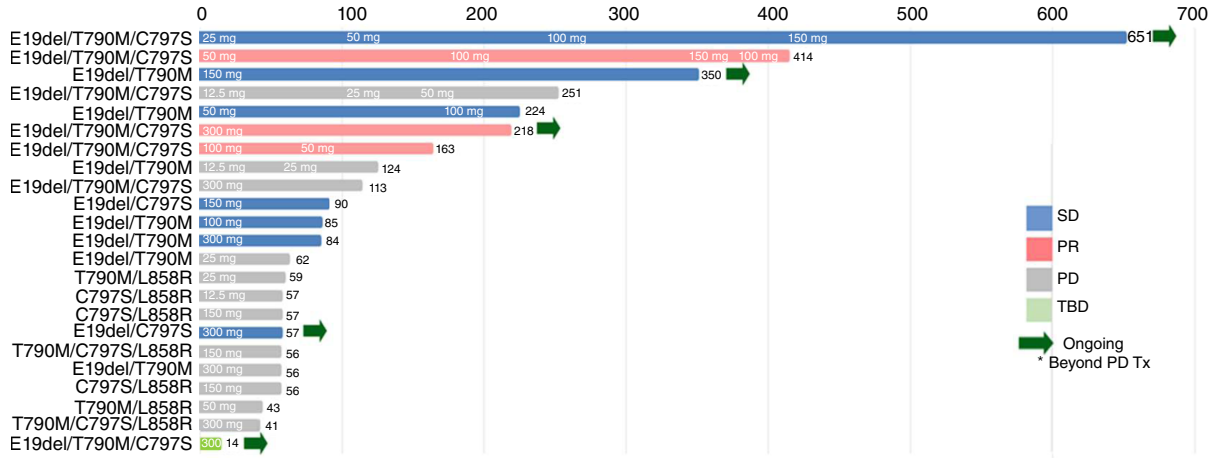

Figure 3.

Swimmer plot showing treatment response in patients receiving JIN-A02 (data cutoff: July 22, 2025). Each horizontal bar represents an individual patient, with the length of the bar indicating treatment duration (days). Colors indicate best overall response [red: PR, blue: SD, gray: PD, and green: to be determined (TBD)]. Arrows indicate patients labeled as ongoing treatment. The X-axis represents treatment duration and the Y-axis lists individual patients along with their EGFR mutation status.

binding of third-generation EGFR TKIs, such as osimertinib (30), thereby rendering them ineffective and significantly limiting subsequent therapeutic options. The clinical complexity is further compounded when C797S emerges alongside T790M, particularly in the cis configuration, in which currently available EGFR TKI combinations have shown limited or no clinical benefit (31).

Extensive efforts are underway to develop next-generation EGFR inhibitors capable of overcoming C797S-mediated resistance. The allosteric inhibitor EAI-045 demonstrated antitumor efficacy in *EGFR* L858R/T790M/C797S mouse models when combined with cetuximab (32), whereas its analogues, JBJ-04-125-02 (33) and JBJ-09-063 (34), exhibited similar mechanisms of action. ATP-competitive inhibitors such as LS-106 (35), CH7233163 (36), and HCD3514 (37) showed high potency and selectivity against triple-mutant *EGFR* in preclinical models. Alternative approaches, including targeted protein degradation via the PROTAC molecule HJM-561 (38) and the macrocyclic inhibitor BI-4020 (39), have also demonstrated preclinical efficacy. Despite these advances, most agents remain at the preclinical stage. Multiple agents targeting the *EGFR* C797S mutation are currently under clinical investigation. BLU-945 (NCT04862780) and BBT176 (NCT04820023) have completed early-phase trials (40, 41), whereas WSD0922-FU (NCT06868485) has entered early-phase trials (42) for *EGFR* C797S–mutant NSCLC. Notably, BH-30643 (NCT06706076), which demonstrated excellent efficacy in preclinical models harboring *EGFR* C797S and atypical *EGFR* mutations, including *EGFR* E20ins, *EGFR* G719A/S768I, and *EGFR* G719A/L861Q, has also begun clinical trials (43).

In this study, we demonstrated that JIN-A02, a fourth-generation EGFR TKI, exhibits potent and selective antitumor activity in preclinical models harboring *EGFR* C797S mutations. JIN-A02 effectively inhibited cell proliferation and suppressed EGFR phosphorylation in both engineered and patient-derived models, including triple-mutant variants containing *EGFR* E19del/T790M/C797S and *EGFR* L858R/T790M/C797S. These effects were consistent across *in vitro* and *in vivo* models, supporting the target specificity of JIN-A02 (**Fig. 1**; Supplementary Fig. S1 and S2). In patient-derived and CRISPR-engineered models, JIN-A02 retained strong antiproliferative activity against *EGFR* C797S–mediated resistance. YU-1097 cells, established from patients with acquired *EGFR* triple mutations following osimertinib therapy, were highly resistant to osimertinib but remained sensitive to JIN-A02. Likewise, JIN-A02 effectively inhibited growth and downstream signaling in PC9_DC cells harboring the *EGFR* E19del/C797S mutation (**Table 2**; Supplementary Fig. S4). These findings validate the efficacy of JIN-A02 across diverse models that represent clinically relevant resistance mechanisms. We report the cellular IC_{90} values to emphasize that durable control of *EGFR*-driven tumors requires deep pathway suppression sufficient to eliminate resistant subpopulations.

It is noteworthy that the effect of JIN-A02 in the triple-mutant model was greater than in the double-mutant model in the colony formation assays whereas JIN-A02 exhibited greater effects on cell viability in the double-mutant model. There may be several explanations underlying this pattern. Colony formation assays (using the triple-mutant YU-1097 model) reflect the long-term proliferative capacity of cancer cells whereas cell viability tests (using the double-mutant PC9 model) exhibit short-term cytotoxicity. The PC9 double-mutant model possesses robust clonogenic recovery capacity, meaning that a subset of persister cells survives drug treatment and can eventually regenerate colonies. Indeed, it has been reported that PC9 cells form drug-tolerant persister populations capable of surviving EGFR inhibition, undergoing reversible cell-cycle arrest, and subsequently resuming proliferation to reconstitute colonies (44). By contrast, the triple-mutant YU-1097 model is a patient-derived cell, which may generally have low intrinsic clonogenic potential, reduced DNA repair fidelity, and high cellular heterogeneity (45). These characteristics of the patient-derived cell may have led to the greater effect of JIN-A02 in the triple-mutant model than in the double-mutant model in the long-term colony formation assays.

In xenograft models established with YU-1097 cells harboring *EGFR* E19del/T790M/C797S mutations, JIN-A02 induced marked and durable tumor regression in a dose-dependent manner. Compared with osimertinib, JIN-A02 achieved greater TGI, with

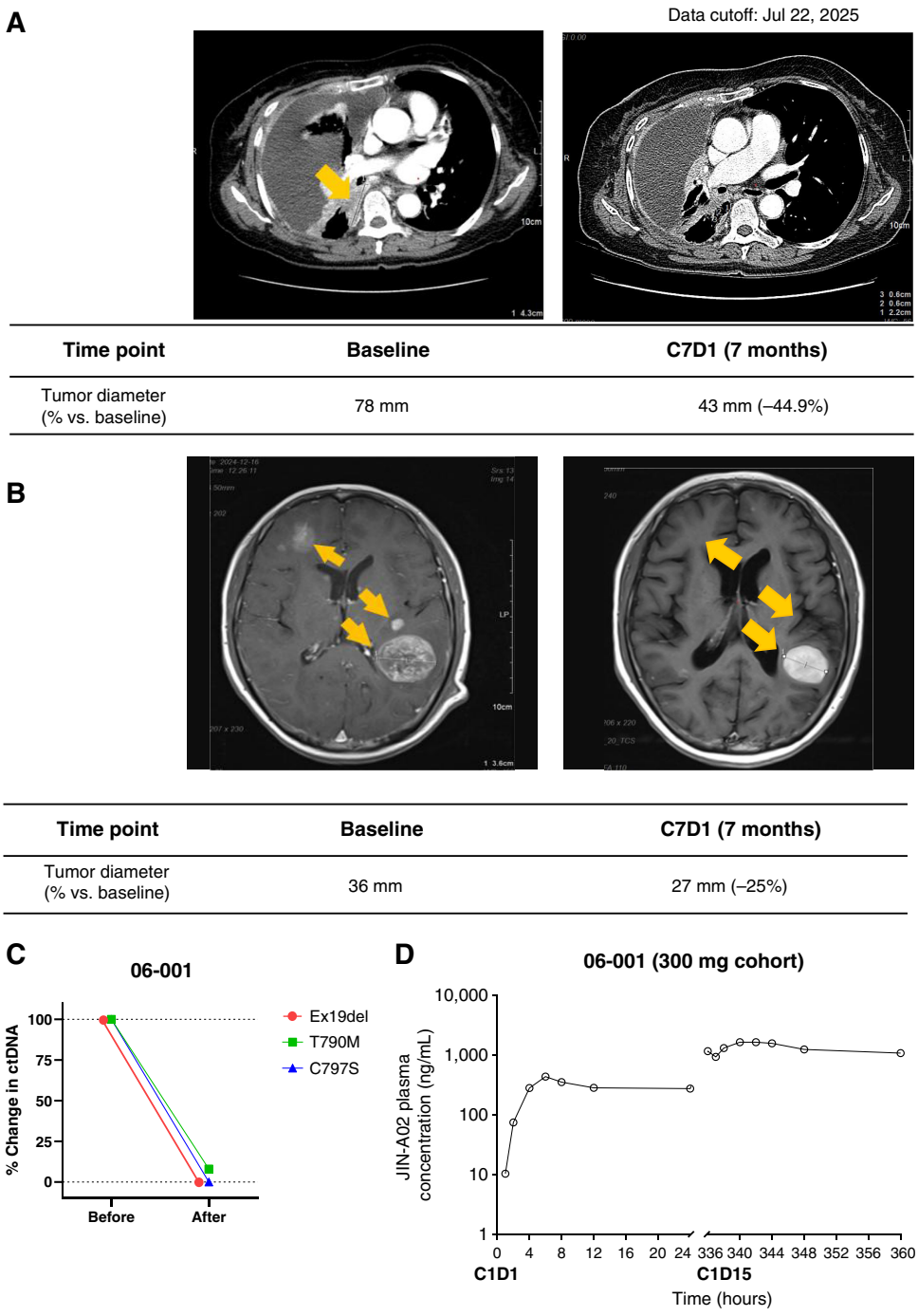

Figure 4.

Activity of JIN-A02 in patients with NSCLC (cohort 6 300 mg). **A,** Target response after JIN-A02 300 mg treatment in a patient with the *EGFR* E19del/T790M/C797S mutation. Orange arrow indicates the tumor lesion. **B,** Intracranial response after JIN-A02 300 mg treatment in a patient with the *EGFR* T790M mutation. Orange arrow indicates the tumor lesion. **C,** Changes in EGFR-mutant ctDNA levels before and after JIN-A02 administration in patients with PR. This figure shows the changes in variant allele frequency levels of EGFR mutations from predose to postdose time points. The relative percentage after dose was calculated by setting predose variant allele frequency levels as 100%. **D,** Plasma concentrations of JIN-A02 from subject 06-001 were analyzed before dose (0) and at 1, 2, 4, 6, 8, 12, and 24 hours after dose following administration of 300 mg JIN-A02 during cycle 1 and cycle 15. C1D1, cycle 1 day 1; C1D15, cycle 1 day 15; C7D1, cycle 7 day 1.

several mice showing complete tumor regression at the 30 mg/kg dose. Importantly, this antitumor effect was achieved without significant changes in body weight, indicating a favorable therapeutic window. Given the clinical relevance of brain metastases in *EGFR*-mutant NSCLC, we further evaluated the intracranial efficacy of JIN-A02 in an orthotopic brain metastasis model. In this model, JIN-A02 significantly suppressed tumor growth as evidenced by bioluminescence imaging, volumetric analysis, and histopathologic examination. Importantly, JIN-A02 treatment resulted in near-complete tumor regression in most animals and was associated with marked tumor clearance in brain tissues.

In the early analysis of a phase I trial involving patients with *EGFR*-mutant NSCLC who experienced disease progression on third-generation EGFR TKI, treatment with JIN-A02 demonstrated favorable safety profile with clinically meaningful activity. Overall, these data support the continued development of JIN-A02 among patients previously treated with EGFR TKI.

In summary, this study demonstrated the preclinical efficacy of JIN-A02 against *EGFR* C797S–mediated resistance, a major clinical obstacle after failure of third-generation EGFR TKIs. Consistent and durable activity across intracranial models highlighted its therapeutic potential. In addition, based on initial analyses from the phase I clinical trial, these findings provide a rationale for continued evaluation of JIN-A02 as a fourth-generation EGFR TKI across diverse clinical settings in treatment-refractory *EGFR*-mutant NSCLC. A limitation of this study includes the single-arm study design and thus the lack of a standard-of-care comparator arm. However, participants had all failed standard-of-care regimens. In addition, the sample size is small to draw a firm conclusion on the activity and tolerability.

Data Availability

The WES data generated from PDCs in this study contain information that could compromise patient privacy and are subject to institutional and regulatory restrictions but are available from the corresponding author upon reasonable request. Processed data relevant to the results, including mutant allele frequency summaries, are provided in the Supplementary Table S1. Additional data supporting the findings of this study were generated by the authors and are available from the corresponding author upon reasonable request.

Authors' Disclosures

K.H. Lee reports grants from Merck and personal fees from Bristol Myers Squibb, MSD, Pfizer, AstraZeneca, Eli Lilly and Company, Yuhan, Daiichi Sankyo, Boehringer Ingelheim, Johnson & Johnson/Janssen, and Amgen outside the submitted work. B.Y. Shim reports grants from Yuhan outside the submitted work. M. Nagasaka reports personal fees from AstraZeneca, Daiichi Sankyo, Eli Lilly and Company, Genentech, Regeneron, Boehringer Ingelheim, Caris Life Sciences, Johnson and Johnson, Pfizer, Bristol Myers Squibb/Mirati Therapeutics, and Takeda and personal fees and other support from AnHeart/Nuvation Bio outside the submitted work. E. Seah reports employment with the Sponsor Company. B.C. Cho reports other support from Champions Oncology, Crown Bioscience, Imagen, Yonsei University Health System, and PearlRiver Bio GmbH; grants from CJ Bioscience, Cyrus, ImmuneOncia, Janssen, J INTS BIO, MSD, Yuhan, Dong-A ST, and LigaChem Bioscience; personal fees from Amgen, ArriVent BioPharma, AstraZeneca, Bristol Myers Squibb, Boehringer Ingelheim, CJ Bioscience, Cyrus Therapeutics, Gilead Sciences, GSK, Regeneron, Janssen, MSD, Yuhan, KANAPH Therapeutics Inc., J INTS Bio, Novartis, and Pfizer; and personal fees and other support from DAAN Biotherapeutics outside the submitted work. S.M. Lim reports grants from Amgen, Yuhan, Beigene, Boehringer Ingelheim, BridgeBio Therapeutics, Oscotec, Roche, GSK, Jiangsu Hengrui, AstraZeneca, Lily, Takeda, Daiichi Sankyo, and J Ints Bio. No disclosures were reported by the other authors.

Authors' Contributions

E.J. Lee: Data curation, software, formal analysis, visualization, writing–review and editing. **J.A. Ko:** Conceptualization, resources, data curation, software, formal analysis, supervision, funding acquisition, validation, investigation, methodology, writing–original draft, project administration, writing–review and editing. **M.-j Kim:** Formal analysis. **J.S. Cho:** Data curation, software, formal analysis, validation, writing–original draft. **J.-Y. Han:** Resources, formal analysis, methodology. **S.W. Kim:** Resources, methodology. **K.H. Lee:** Resources, methodology. **B.Y. Shim:** Resources, methodology. **J.-M. Sun:** Resources, methodology. **M. Nagasaka:** Resources, methodology. **S. Park:** Formal analysis. **S.Y. Oh:** Formal analysis. **M.H. Hong:** Resources, funding acquisition, methodology. **J.B. Lee:** Resources, funding acquisition, methodology. **A. Jo:** Resources, methodology, writing–review and editing. **E. Seah:** Resources, methodology, writing–review and editing. **B.C. Cho:** Resources, funding acquisition, methodology, writing–review and editing. **S.M. Lim:** Conceptualization, resources, data curation, supervision, funding acquisition, investigation, methodology, writing–original draft, project administration, writing–review and editing.

Acknowledgments

This study was supported by the National Research Foundation of Korea grant funded by the Korean Government (RS-2025-005556190 to S.M. Lim and RS-2025-00557272 to B.C. Cho). This research was also supported by a grant (RS-2025-02215737) from the Ministry of Food and Drug Safety in 2025. E.J. Lee was supported by Heo Ji-Young Scholarship Foundation.

Note

Supplementary data for this article are available at Clinical Cancer Research Online (http://clincancerres.aacrjournals.org/).

Received October 2, 2025; revised December 14, 2025; accepted February 4, 2026; posted first February 6, 2026.

References

1. World Health Organization. Global health estimates 2021: deaths by cause, age, sex, by country and by region, 2000–2021. Geneva: World Health Organization; 2024.
2. Surveillance E, End Results Program (SEER). Cancer stat facts: lung and bronchus cancer. [cited 2025 Jul 03]. Available from: https://seer.cancer.gov/statfacts/html/lungb.html.
3. Molina JR, Yang P, Cassivi SD, Schild SE, Adjei AA. Non-small cell lung cancer: epidemiology, risk factors, treatment, and survivorship. Mayo Clin Proc 2008;83:584–94.
4. Levantini E, Maroni G, Del Re M, Tenen DG. EGFR signaling pathway as therapeutic target in human cancers. Semin Cancer Biol 2022;85:253–75.
5. Harrison PT, Vyse S, Huang PH. Rare epidermal growth factor receptor (EGFR) mutations in non-small cell lung cancer. Semin Cancer Biol 2020;61:167–79.
6. Shi Y, Au JS, Thongprasert S, Srinivasan S, Tsai CM, Khoa MT, et al. A prospective, molecular epidemiology study of EGFR mutations in Asian patients with advanced non-small-cell lung cancer of adenocarcinoma histology (PIONEER). J Thorac Oncol 2014;9:154–62.
7. Shigematsu H, Lin L, Takahashi T, Nomura M, Suzuki M, Wistuba II, et al. Clinical and biological features associated with epidermal growth factor receptor gene mutations in lung cancers. J Natl Cancer Inst 2005;97:339–46.
8. Recondo G, Facchinetti F, Olaussen KA, Besse B, Friboulet L. Making the first move in EGFR-driven or ALK-driven NSCLC: first-generation or next-generation TKI? Nat Rev Clin Oncol 2018;15:694–708.
9. Huang YH, Hsu KH, Tseng JS, Chen KC, Hsu CH, Su KY, et al. The association of acquired T790M mutation with clinical characteristics after resistance to first-line epidermal growth factor receptor tyrosine kinase inhibitor in lung adenocarcinoma. Cancer Res Treat 2018;50:1294–303.
10. Soria JC, Ohe Y, Vansteenkiste J, Reungwetwattana T, Chewaskulyong B, Lee KH, et al. Osimertinib in untreated EGFR-mutated advanced non-small-cell lung cancer. N Engl J Med 2018;378:113–25.
11. Mok TS, Wu YL, Ahn MJ, Garassino MC, Kim HR, Ramalingam SS, et al. Osimertinib or platinum-pemetrexed in EGFR T790M-positive lung cancer. N Engl J Med 2017;376:629–40.
12. Ramalingam SS, Vansteenkiste J, Planchard D, Cho BC, Gray JE, Ohe Y, et al. Overall survival with osimertinib in untreated, EGFR-mutated advanced NSCLC. N Engl J Med 2020;382:41–50.
13. Thress KS, Paweletz CP, Felip E, Cho BC, Stetson D, Dougherty B, et al. Acquired EGFR C797S mutation mediates resistance to AZD9291 in non-small cell lung cancer harboring EGFR T790M. Nat Med 2015;21:560–2.
14. Niederst MJ, Hu H, Mulvey HE, Lockerman EL, Garcia AR, Piotrowska Z, et al. The allelic context of the C797S mutation acquired upon treatment with third-generation EGFR inhibitors impacts sensitivity to subsequent treatment strategies. Clin Cancer Res 2015;21:3924–33.
15. Li Y, Mao T, Wang J, Zheng H, Hu Z, Cao P, et al. Toward the next generation EGFR inhibitors: an overview of osimertinib resistance mediated by EGFR mutations in non-small cell lung cancer. Cell Commun Signal 2023;21:71.

16. Leonetti A, Sharma S, Minari R, Perego P, Giovannetti E, Tiseo M. Resistance mechanisms to osimertinib in EGFR-mutated non-small cell lung cancer. Br J Cancer 2019;121:725–37.
17. Mansour MA, AboulMagd AM, Abbas SH, Abdel-Rahman HM, Abdel-Aziz M. Insights into fourth generation selective inhibitors of (C797S) EGFR mutation combating non-small cell lung cancer resistance: a critical review. RSC Adv 2023; 13:18825–53.
18. Kim SY, Lee JY, Kim DH, Joo H, Yun MR, Jung D, et al. Patient-derived cells to guide targeted therapy for advanced lung adenocarcinoma. Sci Rep 2019;9: 19909.
19. Drilon A, Ou S-HI, Cho BC, Kim DW, Lee J, Lin JJ, et al. Repotrectinib (TPX-0005) is a next-generation ROS1/TRK/ALK inhibitor that potently inhibits ROS1/TRK/ ALK solvent- front mutations. Cancer Discov 2018;8:1227–36.
20. Lim SM, Cho BC, Han JY, Kim SW, Lee KH, Nagasaka M, et al. A phase I/II study to evaluate the safety and anti-tumor activity of JIN-A02 in patients with EGFR TKI-refractory, EGFR-mutant advanced NSCLC. Ann Oncol 2023; 34(Suppl 4):S1704–5.
21. Lim SM, Cho BC, Nagasaka M, Reungwetwattana T, Jo A, Seah E, et al. A phase 1, 2 study to evaluate the safety and antitumor activity of JIN-A02 in patients with EGFR mutant advanced NSCLC. J Thorac Oncol 2023;18:S335.
22. Lim SM, Cho BC, Han JY, Kim SW, Lee KH, Nagasaka M, et al. Phase 1/2 clinical trial of JIN-A02, a 4th generation EGFR-tyrosine kinase inhibitor (TKI), in patients with 3rd generation EGFR-TKI resistance in EGFR mutated advanced/metastatic non-small cell lung cancer (NSCLC). Eur J Cancer 2024; 211:S31–2.
23. Lim SM, Cho BC, Han JY, Kim SW, Lee KH, Nagasaka M, et al. Phase 1/2 clinical trial of JIN-A02, a 4th generation EGFR-TKI in EGFR mutated advanced/metastatic non-small cell lung cancer (NSCLC). J Thorac Oncol 2024;19:S346.
24. Lim SM, Cho BC, Han JY, Kim SW, Lee KH, Nagasaka M, et al. Phase 1/2 clinical trial of JIN-A02, a 4th generation EGFR-TKI, in patients with 3rd generation EGFR-TKI resistance in EGFR mutated advanced/metastatic non-small cell lung cancer (NSCLC). Cancer Res 2024;84(Suppl 7):CT154.
25. Lim SM, Cho BC, Han JY, Kim SW, Lee KH, Shim BY, et al. Phase 1/2 clinical trial of JIN-A02, a 4th generation EGFR-TKI in EGFR mutated advanced/metastatic non-small cell lung cancer. Cancer Res 2025;85(Suppl 2): CT184.
26. Lim SM, Cho BC, Han J-Y, Kim S-W, Lee KH, Shim BY, et al. Phase 1/2 clinical trial of JIN-A02, a 4th generation EGFR-TKI in EGFR-mutated advanced/metastatic non-small cell lung cancer. J Clin Oncol 2025;43(Suppl 16):TPS8650.
27. Lim SM, Cho BC, Han J-Y, Kim S-W, Lee KH, Nagasaka M, et al. Phase 1/2 clinical trial of JIN-A02, a 4th generation EGFR-TKI, in patients with 3rd generation EGFR-TKI resistance in EGFR mutated advanced/metastatic non-small cell lung cancer (NSCLC). J Clin Oncol 2024;42:TPS8658.
28. Wang S, Tsui ST, Liu C, Song Y, Liu D. EGFR C797S mutation mediates resistance to third-generation inhibitors in T790M-positive non-small cell lung cancer. J Hematol Oncol 2016;9:59.
29. Zhou X, Zeng L, Huang Z, Ruan Z, Yan H, Zou C, et al. Strategies beyond 3rd EGFR-TKI acquired resistance: opportunities and challenges. Cancer Med 2025;14:e70921.
30. Uchibori K, Inase N, Araki M, Kamada M, Sato S, Okuno Y, et al. Brigatinib combined with anti-EGFR antibody overcomes osimertinib resistance in EGFR-mutated non-small-cell lung cancer. Nat Commun 2017;8:14768.
31. Tan CS, Kumarakulasinghe NB, Huang YQ, Ang YLE, Choo JR, Goh BC, et al. Third generation EGFR TKIs: current data and future directions. Mol Cancer 2018;17:29.
32. Jia Y, Yun CH, Park E, Ercan D, Manuia M, Juarez J, et al. Overcoming EGFR(T790M) and EGFR(C797S) resistance with mutant-selective allosteric inhibitors. Nature 2016;534:129–32.
33. To C, Jang J, Chen T, Park E, Mushajiang M, De Clercq DJH, et al. Single and dual targeting of mutant EGFR with an allosteric inhibitor. Cancer Discov 2019;9:926–43.
34. To C, Beyett TS, Jang J, Feng WW, Bahcall M, Haikala HM, et al. An allosteric inhibitor against the therapy-resistant mutant forms of EGFR in non-small cell lung cancer. Nat Cancer 2022;3:402–17.
35. Liu Y, Lai M, Li S, Wang Y, Feng F, Zhang T, et al. LS-106, a novel EGFR inhibitor targeting C797S, exhibits antitumor activities both in vitro and in vivo. Cancer Sci 2022;113:709–20.
36. Kashima K, Kawauchi H, Tanimura H, Tachibana Y, Chiba T, Torizawa T, et al. CH7233163 overcomes osimertinib-resistant EGFR-Del19/T790M/C797S mutation. Mol Cancer Ther 2020;19:2288–97.
37. Lai M, Zhang T, Chen H, Song P, Tong L, Chen J, et al. Discovery of HCD3514 as a potent EGFR inhibitor against C797S mutation in vitro and in vivo. J Cancer 2023;14:152–62.
38. Du Y, Chen Y, Wang Y, Chen J, Lu X, Zhang L, et al. HJM-561, a potent, selective, and orally bioavailable EGFR PROTAC that overcomes osimertinib-resistant EGFR triple mutations. Mol Cancer Ther 2022;21:1060–6.
39. Suzuki M, Uchibori K, Oh-Hara T, Nomura Y, Suzuki R, Takemoto A, et al. A macrocyclic kinase inhibitor overcomes triple resistant mutations in EGFR-positive lung cancer. NPJ Precis Oncol 2024;8:46.
40. Lim SM, Schalm SS, Lee EJ, Park S, Conti C, Millet YA, et al. BLU-945, a potent and selective next-generation EGFR TKI, has antitumor activity in models of osimertinib-resistant non-small-cell lung cancer. Ther Adv Med Oncol 2024;16:17588359241280689.
41. Lim SM, Fujino T, Kim C, Lee G, Lee YH, Kim DW, et al. BBT-176, a novel fourth-generation tyrosine kinase inhibitor for osimertinib-resistant EGFR mutations in non-small cell lung cancer. Clin Cancer Res 2023;29:3004–16.
42. Conage-Pough JE, Stopka SA, Oh JH, Mladek AC, Burgenske DM, Regan MS, et al. WSD-0922, a novel brain-penetrant inhibitor of epidermal growth factor receptor, promotes survival in glioblastoma mouse models. Neurooncol Adv 2023;5:vdad066.
43. Cui JJ, Rui E, Rogers E, Zhai DY, Jiang P, Wang ZP, et al. Design and discovery of BH-30643: a novel, reversible, mutant-selective macrocyclic EGFR inhibitor invulnerable to common resistance mutations. Cancer Res 2025; 85(Suppl 1):5608.
44. Ramirez M, Rajaram S, Steininger RJ, Osipchuk D, Roth MA, Morinishi LS, et al. Diverse drug-resistance mechanisms can emerge from drug-tolerant cancer persister cells. Nat Commun 2016;7:10690.
45. Arbatskiy M, Balandin D, Churov A, Varachev V, Nikolaeva E, Mitrofanov A, et al. Intratumoral cell heterogeneity in patient-derived glioblastoma cell lines revealed by single-cell RNA-sequencing. Int J Mol Sci 2024;25:8472.